JACS
JOURNAL OF THE AMERICAN CHEMICAL SOCIETY

Communication

pubs.acs.org/JACS

How Half-Coated Janus Particles Enter Cells

Yuan Gao and Yan Yu*

Department of Chemistry, Indiana University, Bloomington, Indiana 47405, United States

Supporting Information

ABSTRACT: Janus particles possess functional asymmetry and directionality within a single entity and thus are predicted to enable many promising biomedical applications that are not offered by homogeneous particles. However, it remains elusive what role the Janus principle plays in Janus particle−cell interactions, particularly in cellular uptake. We studied how asymmetric distribution of ligands on half-coated Janus microparticles dictates the membrane dynamics during receptor-mediated particle uptake, and found key differences from those characteristic of homogeneous particles. Live-cell fluorescence imaging combined with single-particle level quantification of particle−cell membrane interactions shows that the asymmetric distribution of ligands leads to a three-step endocytic process: membrane cup formation on the ligand-coated hemisphere, stalling at the Janus interface, and rapid membrane protrusion on the ligand-absent hemisphere to complete the particle engulfment. The direct correlation between the spatial presentation of ligands on Janus particles and the temporal changes of membrane dynamics revealed in this work elucidates the potential of using the Janus principle to fine-tune particle−cell interactions.

Janus particles, the two-faced particles with different surface makeups on opposing sides, have attracted tremendous attention in the past decade. Their broken symmetry brings distinctive or even incompatible elements (e.g., hydrophobicity/hydrophilicity) into the same structural unit and therefore enables many promising applications, from the formation of colloidal superstructures to biomedical imaging.[1] For example, the combination of synergistic functionalities and multicompartmentalization makes Janus particles particularly attractive as drug delivery vehicles.[2] As the therapeutic efficacy and cytotoxicity of particles are determined by their interactions with cells, understanding how properties of Janus particles influence the particle−cell interactions, particularly cellular uptake of particles, becomes crucial. It is, however, a challenging task due to the complexity of Janus particle−cell interactions. Studies have shown that uptake of particles is governed by their material properties, including size,[3] shape,[3,4] surface chemistry,[5] and mechanical stiffness.[6] However, almost all the existing studies focused on particles that are uniformly functionalized. The anisotropic functionality of Janus particles adds an additional level of complexity. It remains elusive what role the Janus principle plays in particle internalization.

Functional asymmetries (e.g., amphiphilicity of lipids and proteins, polarity of cells) drive the formation of some of the most prominent structures in biological systems and are behind virtually every intracellular process. When a Janus particle whose surface resembles such asymmetries interacts with a cell, a whole new spectrum of behavior is expected, although little has been explored experimentally. Simulation studies have predicted several different modes of interactions between amphiphilic Janus nanoparticles and lipid membranes. The Janus particles, acting like membrane peptides, may stabilize preformed membrane pores, insert into the membrane, or become engulfed by the membrane.[7] Nanoparticles with "striped" surface arrangements of hydrophobic and hydrophilic functional groups, though not the typical half−half Janus geometry, were observed to penetrate cell membranes more efficiently than homogeneous particles.[8] Those studies focused on nonspecific interactions between Janus particles and cells. As specific receptor−ligand binding is more commonly used for targeted particle entry, an important question is how Janus particles displaying anisotropic presentation of ligands cross the cell membrane via receptor-mediated pathways. There is, however, a lack of experimental studies to answer this question. Poon et al. showed that "patchy" nanoparticles that display ligand clusters on the surface enter cells more efficiently than the ones with homogeneous ligand distributions.[9] The underlying connection between ligand presentation and cellular responses, however, is not known. One may speculate similar phenomena for Janus particles that possess asymmetric distribution of ligands. The important question is: what role does the asymmetric functionality of Janus particles play in the cellular uptake process?

In this work, we study how micrometer-sized Janus particles interact with the membrane during their entry into cells, by exploiting the simplest Janus form—only one hemisphere is coated with ligands. We find that the asymmetric distribution of ligands leads to asymmetric membrane cup formation during the receptor-mediated Janus particle uptake. Much differently from a uniformly functionalized particle, a half-coated Janus particle is internalized in a three-step process: a first step involving receptor-mediated membrane wrapping, followed by a membrane stalling step at the Janus interface due to the discontinuity of ligand distribution, and a receptor-independent engulfment at last. The spatial presentation of functionality on Janus particles is shown to directly dictate the temporal dynamics of the cell membrane. We suggest that the half-coated Janus particles switch between different mechanisms on the two hemispheres to enter the cell.

The half-coated Janus particles are 3 μm in diameter and were prepared from monodisperse silica particles (see Figure S1

Received: October 18, 2013
Published: December 5, 2013

dx.doi.org/10.1021/ja410687z | J. Am. Chem. Soc. 2013, 135, 19091−19094

SI and the Experimental Section in SI). One hemisphere was coated with aluminum and passivated with bovine serum albumin (BSA) to prevent nonspecific interactions with cells. Aluminum, whose density (ρ = 2.70 g/cm^3) is close to that of silica particles (ρ = 1.96 g/cm^3), was chosen over other metals to minimize the weight difference between the two hemispheres that may bias the particle orientation. The silica hemisphere was functionalized with anti-CD3 antibodies, which bind T cell receptor complexes on Jurkat cell membranes and lead to receptor-mediated endocytosis.[10] We confirmed in control experiments that the particle uptake events we observed were mediated by ligand−receptor binding (Figure S2 SI). To achieve dual-color confocal imaging of both Janus particles and cells, Jurkat T cell membrane was labeled with a membrane dye, 3,3′-dioctadecyloxacarbo-cyanine perchlorate (DiO), and anti-CD3 molecules were attached onto the Janus particles via streptavidins that were conjugated with Alexa Fluor-568.

A half-coated Janus particle may approach the cell from various orientations. No obvious particle uptake was observed when the metal-coated side faced the cell first, whereas Janus particles were efficiently internalized when the anti-CD3-coated hemisphere first attached to the cell membrane (Figure S3 SI). A representative endocytosis event is illustrated in Figure 1a.

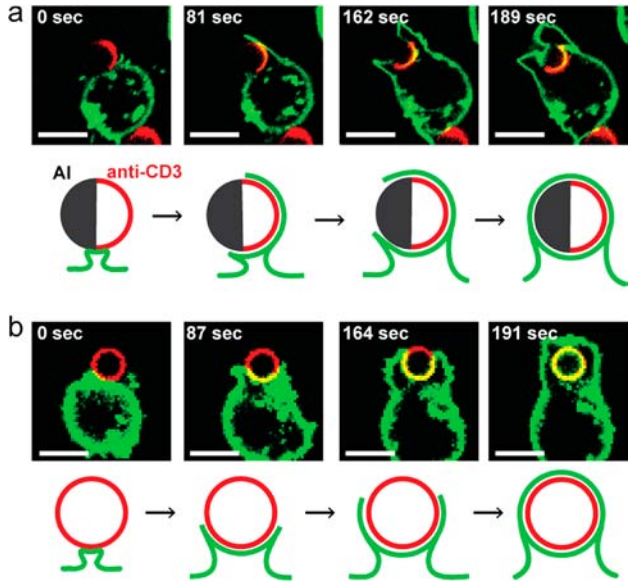

Figure 1. Membrane cup formation is asymmetric during internalization of Janus particles that have ligand anti-CD3 on one hemisphere and metal coating (Al) on the other. Overlay confocal fluorescence images and schematics illustrate membrane protrusion at different elapsed times as indicated during endocytosis of a Janus particle (a) and a uniformly functionalized silica particle (b). In both a and b, Jurkat T cell membranes (labeled with DiO) are shown in green, and streptavidin linkers (labeled with Alexa 568) for anti-CD3 are shown in red. Time zero is set as the time point of initial particle−cell contact. Images are representative of >40 cells for both cases. Scale bars: 5 μm.

Within 1−2 min after the initial particle−cell contact, the membrane rapidly extended around the particle until the entire anti-CD3-coated hemisphere was covered. At the same time, no membrane protruded over the metal-coated hemisphere. Instead, the membrane cup stalled at the Janus boundary, beyond which anti-CD3 is no longer available. The membrane eventually extended rapidly until both sides met to completely engulf the particle. The asymmetric membrane protrusion on the Janus particles was general, but the total time of a complete particle engulfment ranged from 1 to 5 min. The variation, which was also observed with uniformly functionalized particles, is likely due to the intrinsic heterogeneity of cells. To confirm that the asymmetric membrane cup formation is induced by the Janus geometry, we also examined the membrane cup formation during uptake of silica particles that were of the same size as the Janus particles but uniformly functionalized with anti-CD3. We observed that the membrane extended over particles symmetrically throughout the entire particle internalization process (Figure 1b), in agreement with previous reports on endocytosis of homogeneously functionalized particles.[11]

Next, we quantified how membrane protrusion dynamics are correlated with the Janus geometry. We first identified the particle center and the initial particle−cell contact point in each fluorescence confocal image that focused at the particle equator. To quantify membrane protrusion growth in the cross-sectional images, we drew two vectors from the center of the particle to the two rims of the membrane cup. α and β were defined to measure the two angles between either vector and the one from particle center to the initial particle−cell contact point, respectively. Similarly, to quantify the orientation of each Janus particle, α' and β' were defined as the two angles from the initial particle−cell contact point to each Janus interface (see inset in Figure 2b). Figure 2b illustrates how the membrane cup, measured by α and β, grew as a function with time in a representative internalization event of a Janus particle (shown in Figure 2a). Three stages are evident. In the first stage, β increases rapidly with time, while α shows little

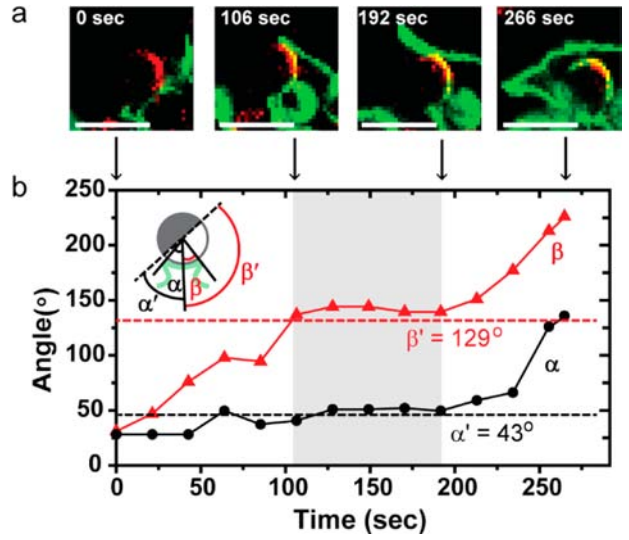

Figure 2. Quantification of the membrane cup formation during endocytosis of a half-coated Janus particle. (a) Overlay confocal fluorescence images of the cell membrane (green) and streptavidin linkers (red) for anti-CD3 at different elapsed times as indicated. (b) Four angles, α, β, α', and β' are defined (inset). In all cross-sectional images, α and β measure the angles from either rim of the membrane cup to the initial particle−cell contact point. α' and β' measure the angles from either Janus interface to the initial particle−cell contact point. α and β obtained from the Janus particle shown in (a) are plotted against time. The plateau region of β is indicated in gray shade. Dotted lines indicate α' and β', which characterize the orientation of the Janus particle. The observation is representative of >40 internalization events. Scale bars: 5 μm.

dx.doi.org/10.1021/ja410687z | J. Am. Chem. Soc. 2013, 135, 19091−19094

change over time, corresponding to the asymmetric cell membrane protrusion. Fluctuation of α around $\alpha' = 43°$ confirms the membrane stalling at the Janus interface. In the second stage, α remains constant, while β reaches a plateau for more than 60 s at around $\beta' = 129°$, where the other Janus interface locates. It shows that once both sides of the membrane cup reach the Janus interface, membrane protrusion stalls completely. In the final stage, both α and β increase rapidly with time, corresponding to fast membrane cup growth from both sides over the nonfunctionalized hemisphere, which eventually leads to the particle engulfment. In contrast, only continuous and symmetric membrane growth was observed for particles that were uniformly functionalized (Figure S4 SI). The membrane stalling at the Janus interface, as clearly demonstrated in the results, indicates that the membrane cup growth during particle internalization is strongly dependent on the ligand distribution. We confirmed that the three-stage endocytic process is a general phenomenon for Janus microparticles of different sizes (Figures S5 and S6 SI).

Surprisingly, the absence of anti-CD3 does not slow down the average membrane growth rate, despite the stalling at the Janus interface. Cell membrane protruded at an average rate of 2.0 ± 1.8 deg/s on the anti-CD3-coated side and at 3.4 ± 2.6 deg/s on the metal-coated side (Figure S7 SI). Membrane dynamics, however, were different on the two hemispheres. In the presence of ligand−receptor binding, the membrane cup tightly conformed to the circumference of the anti-CD3 side, similarly as on uniformly functionalized particles (Figure S8 SI). However, the cell membrane underwent large fluctuations such as rapid elongation and retraction when it extended over the metal-coated side. As a result, Janus particles were engulfed into spacious membrane cups larger than the particle size (Figures 3 and S8 in SI). In contrast, membrane cups around homogeneous particles were tight-fitting. The distinct membrane dynamics suggest that internalization of the half-coated Janus particles may involve multiple mechanisms, depending on the availability of ligand−receptor binding. As actin polymerization is known to be one of the major driving forces for particle endocytosis,[12] we next investigated whether the asymmetric distribution of ligands on the Janus particles leads to different actin assembly in the membrane cups. As anti-CD3 binding to T cell receptors triggers actin polymerization in Jurkat T cells,[13] one might expect that the absence of anti-CD3 leads to reduced or diminished actin assembly. Our results, however, suggest otherwise. As illustrated in Figure 3, actin, stained with fluorescently labeled phalloidin in fixed Jurkat cells, accumulated in the membrane cups at all stages of the particle uptake. It suggests that actin is likely involved in the membrane protrusion even without any local signals from anti-CD3 binding to T cell receptors.

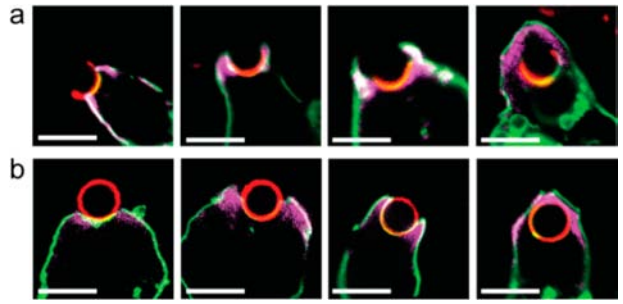

Figure 3. Actin accumulates in membrane cups for both Janus particles (a) and uniformly functionalized particles (b). Overlay confocal fluorescence images of actin (magenta), Jurkat T cell membrane (green), and streptavidin linkers (red) for anti-CD3 in fixed Jurkat T cells. Each image is representative of 5−25 cells that were observed at each endocytic stage. Scale bars: 5 μm.

To further investigate the role of asymmetric functionalization in Janus particle uptake, we analyzed the overall internalization percentage of Janus particles and control particles that were uniformly functionalized as a function of ligand surface density. The surface density of anti-CD3 was varied from 0 to approximately 250 molecules/μm^2 and measured with the quantitative fluorescence method (see the Experimental Section in SI). We found that for both Janus particles and control particles, percentage of internalization increased at higher anti-CD3 surface densities, in agreement with previous reports.[14] At the same anti-CD3 surface density, a smaller fraction of Janus particles were internalized than control particles (Figure 4a), likely due to the effect of particle orientation—a Janus particle with the metal-coated side facing the cell initially is less likely to be uptaken (Figure S3 SI). Interestingly, the effect of Janus geometry became negligible when the total number of ligands on the particle surface was kept constant (Figure 4b). It is possible that the effect from the increased ligand density counteracts that of the Janus particle orientation.

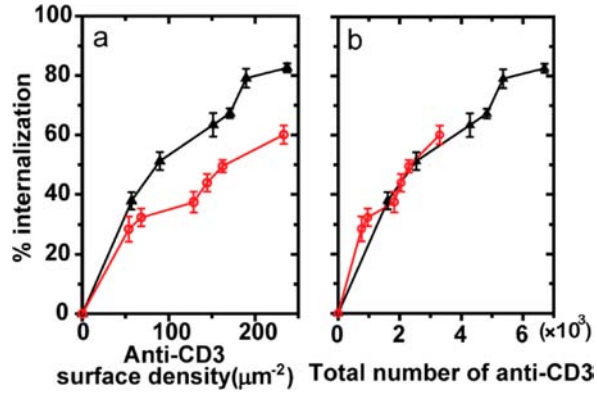

Figure 4. Internalization efficiency of Janus particles is dependent on ligand density and Janus geometry. Percent internalization for Janus particles (red ○) and uniformly functionalized particles (black ▲) is plotted against anti-CD3 surface density (panel a) and the total number of anti-CD3 on particle surfaces (panel b).

Two main mechanisms (zipper model and trigger model) have been proposed for internalization of large particles (also known as phagocytosis),[11] but neither can completely explain our observations. The zipper model proposes that particle engulfment occurs via zipper-like engagement of the cell membrane against the particle surface and stops in the absence of ligand−receptor binding.[15] In contrast, the trigger model is an "all-or-none" mechanism: the initial particle−cell binding, if above a certain threshold signal strength, is sufficient for complete uptake of the particle.[11a] The eventual internalization of half-coated Janus particles in this study clearly contradicts the prediction of the zipper model. Instead, the distinctive membrane morphology on the two hemispheres suggests that the half-coated Janus particles might exploit a combination of zipper and trigger mechanisms to enter cells—the close-fitting membrane cup and successive protrusion on the anti-CD3-

dx.doi.org/10.1021/ja410687z | J. Am. Chem. Soc. 2013, 135, 19091−19094

coated hemisphere are characteristic of the zipper model, while the large membrane fluctuation and rapid membrane extension without ligand−receptor binding on the nonfunctionalized hemisphere seem to agree with the trigger model. To identify the exact mechanisms underlying the Janus particle internalization, which is beyond the scope of this report, details of the biochemical signaling pathways will need to be investigated.

In summary, we show in this study how asymmetric distribution of ligands on half-coated Janus particles dictates the cell membrane to regulate receptor-mediated particle uptake. Unlike particles that are uniformly functionalized, micrometer-sized Janus particles with ligands coated on one hemisphere enter cells in a three-step process: membrane protrusion on the ligand-coated hemisphere, stalling at the Janus interface, and rapid membrane extension on the ligand-absent hemisphere to complete the particle engulfment. The asymmetric distribution of ligands has little effect on localized assembly of actin in the membrane cups, but influences membrane dynamics. Membrane protrusion tightly conforms to the particle shape on the anti-CD3-coated side but exhibits large fluctuations on the nonfunctionalized side. In addition, the asymmetric functionalization of Janus particles reduces the overall particle internalization efficiency, but its effect may be counteracted by increasing ligand surface density. Our results uncover the direct correlation between the spatial presentation of ligands on Janus microparticles and membrane dynamics during particle uptake. This work demonstrates how the Janus geometry may be used as a new design principle to fine-tune particle−cell interactions. It is important to note that some cell types also internalize microparticles nonspecifically in addition to specific receptor-mediated pathways.[16] It will be important in future studies to investigate how half-coated Janus particles navigate between both pathways during endocytosis in those cells.

■ ASSOCIATED CONTENT

Supporting Information

Experimental section, data showing characterization of Janus particles, quantification of Janus particle endocytosis, supporting fluorescence confocal images. This material is available free of charge via the Internet at http://pubs.acs.org.

■ AUTHOR INFORMATION

Corresponding Author

yy33@indiana.edu

Notes

The authors declare no competing financial interest.

■ ACKNOWLEDGMENTS

We thank Jim Powers of the IUB Light Microscopy Imaging Center for fluorescence imaging assistance, Dr. Yi Yi of the Indiana University Nanoscale Characterization Facility for assistance with SEM and thermal evaporator, Prof. Charles Dann III for the use of NanoDrop, Prof. Richard DiMarchi for the use of lyophilizer, Dr. John Hammer III (National Institutes of Health) for anti-CD3 labeling protocol, and Indiana University for funding.

■ REFERENCES

(1) (a) Chen, Q.; Bae, S. C.; Granick, S. *J. Am. Chem. Soc.* **2012**, *134*, 11080. (b) Walther, A.; Müller, A. H. E. *Chem. Rev.* **2013**, *113*, 5194. (c) Lee, S.-M.; Kim, H. J.; Ha, Y.-J.; Park, Y. N.; Lee, S.-K.; Park, Y.-B.; Yoo, K.-H. *ACS Nano* **2013**, *7*, 50. (d) Lv, W.; Lee, K. J.; Li, J.; Park, T.-H.; Hwang, S.; Hart, A. J.; Zhang, F.; Lahann, J. *Small* **2012**, *8*, 3116. (e) Hu, S.-H.; Gao, X. *J. Am. Chem. Soc.* **2010**, *132*, 7234. (f) Yoshida, M.; Roh, K.-H.; Mandal, S.; Bhaskar, S.; Lim, D.; Nandivada, H.; Deng, X.; Lahann, J. *Adv. Mater.* **2009**, *21*, 4920. (g) Wu, L. Y.; Ross, B. M.; Hong, S.; Lee, L. P. *Small* **2010**, *6*, 503. (h) Suci, P. A.; Kang, S.; Young, M.; Douglas, T. *J. Am. Chem. Soc.* **2009**, *131*, 9164.

(2) (a) Rahmani, S.; Park, T.-H.; Dishman, A. F.; Lahann, J. *J. Controlled Release* **2013**, *172*, 239. (b) Hwang, S.; Lahann, J. *Macromol. Rapid Commun.* **2012**, *33*, 1178. (c) Misra, A. C.; Bhaskar, S.; Clay, N.; Lahann, J. *Adv. Mater.* **2012**, *24*, 3850.

(3) Gratton, S. E. A.; Ropp, P. A.; Pohlhaus, P. D.; Luft, J. C.; Madden, V. J.; Napier, M. E.; DeSimone, J. M. *Proc. Natl. Acad. Sci. U.S.A.* **2008**, *105*, 11613.

(4) Doshi, N.; Mitragotri, S. *PLoS One* **2010**, *5*, e10051.

(5) (a) Saha, K.; Kim, S. T.; Yan, B.; Miranda, O. R.; Alfonso, F. S.; Shlosman, D.; Rotello, V. M. *Small* **2013**, *9*, 300. (b) Moyano, D. F.; Goldsmith, M.; Solfiell, D. J.; Landesman-Milo, D.; Miranda, O. R.; Peer, D.; Rotello, V. M. *J. Am. Chem. Soc.* **2012**, *134*, 3965.

(6) Merkel, T. J.; Jones, S. W.; Herlihy, K. P.; Kersey, F. R.; Shields, A. R.; Napier, M.; Luft, J. C.; Wu, H.; Zamboni, W. C.; Wang, A. Z.; Bear, J. E.; DeSimone, J. M. *Proc. Natl. Acad. Sci. U.S.A.* **2011**, *108*, 586.

(7) (a) Alexeev, A.; Uspal, W. E.; Balazs, A. C. *ACS Nano* **2008**, *2*, 1117. (b) Ding, H.; Ma, Y. *Nanoscale* **2012**, *4*, 1116.

(8) (a) Verma, A.; Uzun, O.; Hu, Y.; Hu, Y.; Han, H.-S.; Watson, N.; Chen, S.; Irvine, D. J.; Stellacci, F. *Nat. Mater.* **2008**, *7*, 588. (b) Jewell, C. M.; Jung, J.-M.; Atukorale, P. U.; Carney, R. P.; Stellacci, F.; Irvine, D. J. *Angew. Chem., Int. Ed.* **2011**, *50*, 12312.

(9) Poon, Z.; Chen, S.; Engler, A. C.; Lee, H.-i.; Atas, E.; von Maltzahn, G.; Bhatia, S. N.; Hammond, P. T. *Angew. Chem., Int. Ed.* **2010**, *49*, 7266.

(10) Borroto, A.; Lama, J.; Niedergang, F.; Dautry-Varsat, A.; Alarcón, B.; Alcover, A. *J. Immunol.* **1999**, *163*, 25.

(11) (a) Swanson, J. A. *Nat. Rev. Mol. Cell Biol.* **2008**, *9*, 639. (b) Flannagan, R. S.; Jaumouille, V.; Grinstein, S. *Annu. Rev. Pathol.: Mech. Dis.* **2012**, *7*, 61.

(12) Mooren, O. L.; Galletta, B. J.; Cooper, J. A. *Annu. Rev. Biochem.* **2012**, *81*, 661.

(13) (a) Fuller, C. L.; Braciale, V. L.; Samelson, L. E. *Immunol. Rev.* **2003**, *191*, 220. (b) Gomez, T. S.; Billadeau, D. D. *Adv. Immunol.* **2008**, *97*, 1.

(14) (a) Bandyopadhyay, A.; Fine, R. L.; Demento, S.; Bockenstedt, L. K.; Fahmy, T. M. *Biomaterials* **2011**, *32*, 3094. (b) Pacheco, P.; White, D.; Sulchek, T. *PLoS One* **2013**, *8*, e60989.

(15) Griffin, F. M.; Griffin, J. A.; Leider, J. E.; Silverstein, S. C. *J. Exp. Med.* **1975**, *142*, 1263.

(16) Champion, J. A.; Mitragotri, S. *Proc. Natl. Acad. Sci. U.S.A.* **2006**, *103*, 4930.